Material Discrimination by High-Energy X-Ray Dual-Energy Imaging

WANG Xue-Wu[1)] LI Jian-Min KANG Ke-Jun TANG Chuan-Xiang ZHANG Li
CHEN Zhi-Qiang LI Yuan-Jing ZHONG Hua-Qiang

(Department of Engineering Physics, Tsinghua University, Beijing 100084, China)

Abstract Material discrimination by high-energy (1—10MeV) X-ray dual-energy imaging is investigated in this paper, and an approximately linear model is also proposed. The sensitivity of material discrimination is defined to evaluate the effect of material discrimination. The energy ranges of dual-energy X-ray are optimized by analyzing the X-ray attenuation coefficients after the X-ray penetrate the materials. The sensitivity of material discrimination can be improved by modulating the X-ray energy spectrum with filters. A prototype emitting alternating dual-energy X-ray with 9MeV & 6MeV boundary energies is designed. It can present us the tinctorial images with the material discrimination information. Finally, the experimental results we made agree with the theoretical simulation.

Key words high-energy X-ray imaging, dual-energy imaging, material discrimination, LINAC, energy spectrum modulation

1 Introduction

By weighing the difference in attenuation coefficients between organic and inorganic materials for high and low energy X-ray, the dual-energy method has been widely applied in luggage X-ray inspection systems for the purpose of material discrimination[1—8]. Recently, the dual-energy method begins to be prevalent in the high-energy X-ray imaging container inspection systems for discriminating the materials of the cargo since the container inspection systems are widely deployed all over the world.

The typical boundary energy of X-ray used in luggage systems does not exceed 200keV, which is in the domain of photoelectric interactions. Consequently, the X-ray attenuation coefficient strongly depends on the atomic number of the matter needed to be scanned, so material discrimination can be easily realized. However, the boundary energy of X-ray used in container inspection system is 1—10MeV. But the attenuation coefficient of the high penetration X-ray is barely correlated with the atomic number, which hardly achieves material discrimination[9].

Though the difficulty impedes the dual-energy imaging in high energy X-ray domain, this technology has been applied in high-energy X-ray imaging systems, in which specially designed detector and spectral filter are needed to be elaborated[10—12], and interlaced dual-energy X-ray pulses from LINAC are used[13—25]. But the interlaced dual-energy X-ray may cause the problems of the low sensitivity of material discrimination and the wrong discrimination of the thin objects.

In this study, the physical principle of material discrimination by high-energy X-ray dual-energy imaging is extensively studied. A mathematic processing model is also revised to be approximately

Received 14 March 2007

1) E-mail: wangxuewu@tsinghua.edu.cn

linear. The sensitivity of material discrimination (SMD) is defined in order to rank the performance of material discrimination. The method of setting the optimal energy ranges of dual-energy X-ray is also introduced, together with an experiment of energy spectrum modulation of dual-energy X-ray demonstrating the improvement of the SMD and offering an effective solution for the incompetence of the discrimination of the thin objects.

A prototype using interlaced dual-energy X-ray with 9MeV & 6MeV boundary energies is made and tinctorial images with material discrimination information are obtained. The results of experiments show strong agreement with the theoretical analysis and simulation.

2 Physical background

Transparency is defined as the ratio between two quantities of the radiation intensity after and before the penetration of an object. $T(E_{\mathrm{H}},t,Z)$ and $T(E_{\mathrm{L}},t,Z)$ are transparencies of the material with atomic number Z and thickness t. The quantitative expression of T is given by Eq. (1).

$$\begin{cases} T_{\mathrm{H}}=T(E_{\mathrm{H}},t,Z)=\dfrac{D_{\mathrm{H}}}{D_{\mathrm{H0}}}= \\ \qquad \dfrac{\displaystyle\int_0^{E_{\mathrm{H}}}\frac{\mathrm{d}P_{\mathrm{H}}}{\mathrm{d}E}(E_{\mathrm{H}},E)\cdot \mathrm{e}^{-\mu(E,Z)t}\cdot \mathrm{d}E}{\displaystyle\int_0^{E_{\mathrm{H}}}\frac{\mathrm{d}P_{\mathrm{H}}}{\mathrm{d}E}(E_{\mathrm{H}},E)\cdot \mathrm{d}E}, \\ T_{\mathrm{L}}=T(E_{\mathrm{L}},t,Z)=\dfrac{D_{\mathrm{L}}}{D_{\mathrm{L0}}}= \\ \qquad \dfrac{\displaystyle\int_0^{E_{\mathrm{L}}}\frac{\mathrm{d}P_{\mathrm{L}}}{\mathrm{d}E}(E_{\mathrm{L}},E)\cdot \mathrm{e}^{-\mu(E,Z)t}\cdot \mathrm{d}E}{\displaystyle\int_0^{E_{\mathrm{L}}}\frac{\mathrm{d}P_{\mathrm{L}}}{\mathrm{d}E}(E_{\mathrm{L}},E)\cdot \mathrm{d}E}. \end{cases} \tag{1}$$

where E_{H} and E_{L} are the boundary energies with respect to two X-ray beams, $P(E_{\mathrm{H}},E)$ and $P(E_{\mathrm{L}},E)$ are their energy distributions, D_{H0}, D_{H} and D_{L0}, D_{L} are the radiation intensity of high and low energy X-ray before and after the penetration of the object respectively, and $\mu(E,Z)$ is the attenuation coefficient of the material with respect to the atomic number Z and photon energy E.

The α-curve model[13] is described as Eq. (2):

$$\begin{cases} x=\ \alpha_{\mathrm{H}}=(-\ln T_{\mathrm{H}}) \\ y=\ \alpha_{\mathrm{L}}-\alpha_{\mathrm{H}}=(\ln T_{\mathrm{H}}-\ln T_{\mathrm{L}}). \end{cases} \tag{2}$$

The sensitivity of material discrimination (SMD) based on the α-curve analysis is used to evaluate the effect of material discrimination. Therefore, the SMD of two materials with atomic number Z_1 and Z_2 at a fixed value α_{H} can be expressed as:

$$D(Z_1,Z_2,\alpha_{\mathrm{H}})=y(Z_1,\alpha_{\mathrm{H}})-y(Z_2,\alpha_{\mathrm{H}}). \tag{3}$$

where $y(Z_1,\alpha_{\mathrm{H}})$ and $y(Z_2,\alpha_{\mathrm{H}})$ are respectively the y-axis value of material Z_1 and Z_2 at α_{H} in the α-curve coordinate. The two materials can be easily differentiated if their α-curves are largely separated. On the contrary, the materials cannot be differentiated easily if their α-curves are too close. So, the greater the absolute value of the SMD, the easier the discrimanation of the two materials.

3 Optimizing energy spectrum

Equation (2) can be rewritten as:

$$\begin{cases} x=\ -\ln T_{\mathrm{H}}=\bar{\mu}_{\mathrm{eff}}(E_{\mathrm{H}},t,Z)\cdot t \\ y=\ \ln T_{\mathrm{H}}-\ln T_{\mathrm{L}}=(\bar{\mu}_{\mathrm{eff}}(E_{\mathrm{L}},t,Z)- \\ \qquad \bar{\mu}_{\mathrm{eff}}(E_{\mathrm{H}},t,Z))\cdot t\,. \end{cases} \tag{4}$$

where $\bar{\mu}_{\mathrm{eff}}(E_{\mathrm{H}},t,Z)$ and $\bar{\mu}_{\mathrm{eff}}(E_{\mathrm{L}},t,Z)$ are the effective attenuation coefficients of the material at high and low energy X-ray. If the thickness of the penetrated object increases gradually, the X-ray will be gradually hardened, so the effective attenuation coefficient will become smaller and smaller.

Substituting Eq. (4) into (3), we get:

$$D(Z_1,Z_2,\alpha_{\mathrm{H}})\propto\big((\bar{\mu}_{\mathrm{eff-L-}Z_1}-\bar{\mu}_{\mathrm{eff-L-}Z_2})- \\ (\bar{\mu}_{\mathrm{eff-H-}Z_1}-\bar{\mu}_{\mathrm{eff-H-}Z_2})\big)\cdot t\,. \tag{5}$$

where four new signs $\bar{\mu}_{\mathrm{eff-H-}Z_1}$, $\bar{\mu}_{\mathrm{eff-L-}Z_1}$ and $\bar{\mu}_{\mathrm{eff-H-}Z_2}$, $\bar{\mu}_{\mathrm{eff-L-}Z_2}$ are the effective attenuation coefficients of material Z_1, Z_2 at high and low energy X-ray.

So, Eq. (5) is the foundation of the determination of the optimal energy range. Some typical materials are selected to describe the implication of Eq. (5). The differences of mass attenuation coefficients between organic and inorganic materials as well as the ones between inorganic and high-Z materials are shown in Fig. 1[26]. The maximum difference of the effective attenuation coefficients between two energies can be regarded as the criteria for the optimal energy range. As shown in Fig. 1, the peak is shown in the low energy area, but it decreases along with the energy axis. Therefore, theoretically, the selection of optimal value of low energy X-ray should be around the peak. But for the high energy X-ray, the highest value is what we should select. According to Fig. 1, in order to optimize the energy spectrum for improving the effect of material discrimination, the photon energy range of high energy X-ray should be set above 4MeV. The rule of high energy selection is that the higher the energy, the better the effect. But the optimal range for low energy X-ray depends on the materials to be differentiated. If the organic & inorganic materials need to be differentiated, 0.3—3MeV is the optimal energy range, but the optimal energy range is 1—4MeV if the inorganic & high-Z materials require to be differentiated.

Figure 1 also indicates that the photons with the energy lower than the optimal energy range of low energy X-ray will depress material discrimination when the object is thin, which also is the reason why the thin objects cannot be well differentiated.

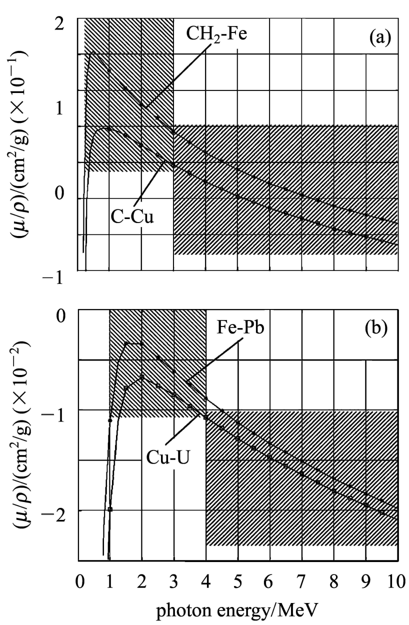

Fig. 1. Difference of μ/ρ between organic and inorganic materials (a), as well as inorganic and high-Z materials (b). Shadings represent the optimal energy ranges of low and high energy X-ray respectively.

4 Energy spectrum modulation

High-Z materials, such as Pb, W and U, are often used as spectral filter[27]. The energy distributions of both high energy X-ray (9MeV) and low energy X-ray (4MeV) modulated by different filters are simulated and normalized, as presented in Fig. 2. The original energy spectra are also simulated by MCNP 4B and normalized.

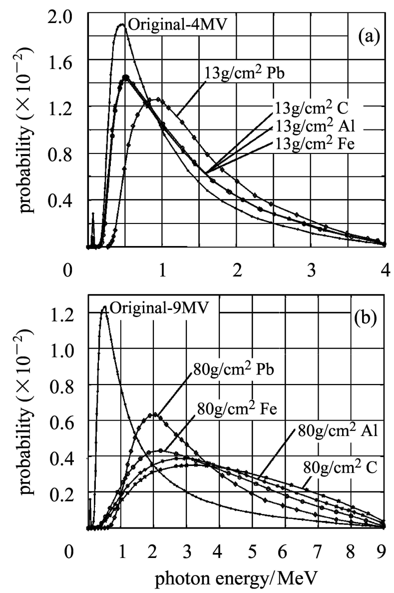

Fig. 2. The effect of spectrum modulation by different materials with the 4MV low energy X-ray (a) and 9MV high energy X-ray (b).

The comparison between Fig. 1 and Fig. 2 shows the accordance between the energy spectrum modulation and the optimal energy range. From the figures, the spectrum curves of the high-Z materials are separated farther in the low energy range of the X-ray, but the ones of the low-Z materials are separated farther in the high energy range of the X-ray. The reason is due to the predomination of photoelectric interaction between high-Z material and low energy X-ray with energy lower than the optimal energy range, and lack of pair production between low-Z material and high energy X-ray in the optimal energy range.

The SMD value is greater as the mass thickness of modulation material increases for most of the materials. The SMD of thin inorganic and high-Z materials as well as the differentiation capability of thin materials will be greatly improved when 3—5g/cm^2 Pb is used to modulate low energy X-ray. Furthermore, the SMD will be improved 100%—200% when 60—80g/cm^2 CH_2 or C is used to modulate high energy X-ray, as shown in Fig. 3. But the intensity reduction of X-ray after the spectrum modulation will lead to the degradation of the inspection image quality as well as signal-to-noise (SNR). As a consequence, it might affect the accuracy of material discrimination somewhat. However, taking into account the great enhancement of SMD, the negative effect caused by intensity loss can be limited to an acceptable extent. For example, the intensity of 9MV X-ray decreases only to around 1/8 after it is modulated by the 60g/cm^2 graphite, but the testing data shows that penetration can still reach about 380mm iron after spectrum modulation process. For achieving the best modulated spectrum, the most appropriate mass thickness of modulating material should be carefully tested, but it varies with practical applications.

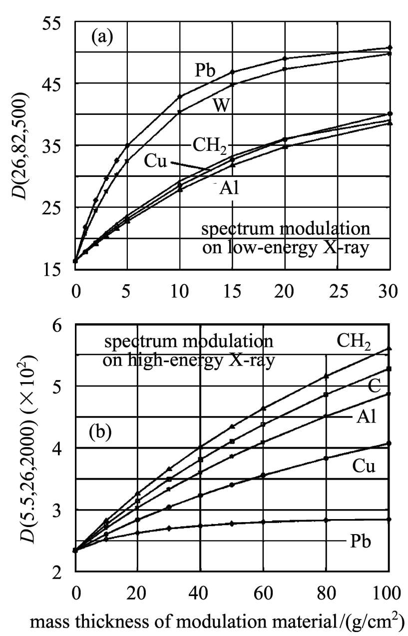

Fig. 3. Influence on SMD by spectrum modulation on low and high energy X-ray. (a) The boundary energy used for spectrum modulation on low energy X-ray is 5MeV. D (26, 82, 500) is SMD of Fe/Pb on α_H=500. (b) The boundary energy used for spectrum modulation on high energy X-ray is 9MeV. D (5.5, 26, 2000) is SMD of CH_2/Fe on α_H=2000.

5 Experiments

Experiments were performed on the high-energy X-ray imaging experimental system in the accelerator lab of Tsinghua University. The LINAC consists of a 9MeV standing wave accelerating tube, a MG5193 magnetic tube and MG6062 electromagnet. The collimating system can reshape the X-ray beam to an 8mm-wide fan-shaped X-ray beam. A detector array mainly made of the 6mm×6mm $CdWO_4$ pitch is used to detect X-ray. The facility for the spectrum modulation is close to the accelerator. The composition of the system is illustrated in Fig. 4.

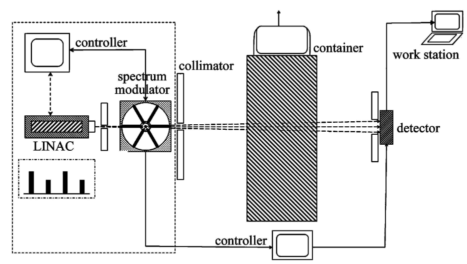

Fig. 4. Composition of the experimental system.

The X-ray beams with different boundary energies, calibrated by means of measuring the half-value layer, are obtained by changing the intensity of electron beam and micro-wave power. The experimental α-curves of the typical materials, such as CH_2, Fe and Pb, are plotted in Fig. 5, which are obtained on the prototype with X-ray with 9MeV & 6MeV boundary energies and about 1000cGy/min·m@80pps output intensity. The results of the SMD before and after spectrum modulation on both high and low energy X-ray are depicted in Fig. 6, which agree with the above theoretical analysis and simulation.

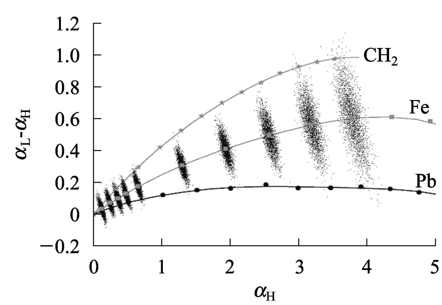

Fig. 5. α-curves of typical materials on the prototype with 9MeV & 6MeV boundary energies.

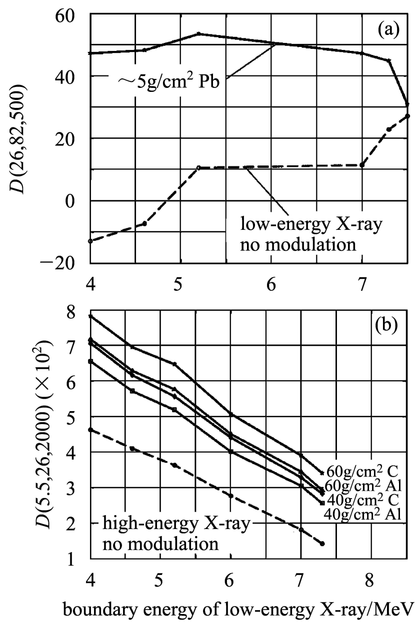

Fig. 6. Experimental SMD before and after spectrum modulation both on low energy (a) and high energy (b) X-ray. The boundary energies of low and high energy X-ray are 5MeV and 9MeV respectively. D (26, 82, 500) and D (5.5, 26, 2000) are SMD of Fe/Pb on $\alpha_{\rm H}$=500 and SMD of CH_2/Fe on $\alpha_{\rm H}$=2000 respectively.

In imaging experiments, LINAC alternately emits X-ray beams with the boundary energies 9MeV & 6MeV by changing the intensity of electron beam and micro-wave power. The facility of spectrum modulation can synchronously modulate high and low energy X-ray while objects are moved smoothly. Signals are detected by the detector array and sent to the image processing station. Both the grey images and tinctorial images containing material discrimination information are gained.

6 Conclusions

The physical principle of material discrimination by high-energy X-ray dual-energy imaging has been investigated, and the α-curve model revised to be a more practical format. The SMD is defined based on the α-curve model, which is useful for evaluating the effect of material discrimination. The treatment of optimizing energy spectrum of dual-energy X-ray is to find the optimal energy range of both high and low energy X-ray for differentiating different materials. The experiments demonstrate that in the optimal energy range, the thick low-Z material used for high energy spectrum modulation of the X-ray and the thin high-Z material used for the low energy spectrum modulation of the X-ray could improve the SMD and offer the differentiation ability of thin object. A prototype using interlaced dual-energy X-ray with 9MeV & 6MeV boundary energies is fabricated. Tinctorial images with material discrimination information are collected. The results of experiments show a strong agreement with the theoretical analysis and simulation.

The SMD of the dual-energy method in high-energy X-ray imaging system is greatly improved in this study, which pushes the progress of this technology in the large cargo inspection area. But there still are some issues which need to be considered. (1) The SMD should be considered together with SNR to accurately assess the final realization effect of material discrimination. (2) The dual-energy method is insufficient while optimizing energy ranges is different for the differentiation of different materials. (3) The spectral response of the detector is a valuable topic besides X-ray source and spectrum modulation. (4) A better revised α-curve model or a new model continues to be under investigation. The enhancement of SMD is always the crucial issue of material discrimination by high-energy X-ray dual-energy imaging.

References

1 http://www.smithsdetection.com
2 http://www.l-3com.com
3 http://www.rapiscansystems.com
4 http://www.as-e.com
5 http://www.nuctech.com
6 http://www.fri.com.cn
7 http://www.gesecurity.com
8 LU Qiang. The Utility of X-ray Dual-Energy Transmission and Scatter Technologies for Illicit Material Detection. PhD Dissertation. Virginia Tech, 1999
9 Moore J F, Ravichandran V C, Reiter R F. Port Technology International, 2001, **10**: 113—119
10 Neale W W, Rushbrooke J G, Ansorge R E. U.S. Patent, 1996, US 5,524,133
11 Perion D, Martin T, Maitrejean S et al. PCT Patent, 2000,

WO 00/43760
12 Bjorkholm P J. U.S. Patent, 2000, US 6,069,936
13 Novikov V L, Ogorodnikov S A, Petrunin V I. Dual Energy Method of Material Recognition in High Energy Introscopy Systems. In: International Workshop on Charged Particle Linear Accelerators: Problems of Atomic Science and Technology, 1999. 93—95
14 Ogorodnikov S A, Petrunin V I, Vorogushin M F. Application of High-Penetrating Introscopy Systems for Recognition of Materials. In: Proceedings of the 7th EPAC. Vienna, 2000. 2583—2585
15 Ogorodnikov S A, Petrunin V I. Processing of Interlaced Images in 4—10 MeV Dual Energy Customs System for Material Recognition. In: Proceedings of the 6th International Computional Accelerator Physics Conference. Darmstadt, Germany, 2000
16 Vorogushin M F, Ogorodnikov S A, Petrunin V I. Experiments on Material Recognition for 8MeV Customs Inspection System for Trucks and Large-Scale Containers. In: Proceedings of the 20th International Linac Conference. 2000. 642—644
17 Ogorodnikov S A, Petrunin V I. Physical Review Special Topics—Accelerators and Beams, 2002, **5**(104701): 1—11
18 Ogorodnikov S A, Petrunin V I, Vorogushin M F. Radioscopic Discrimination of Materials in 1—10MeV Range for Customs Applications. In: Proceedings of the 8th EPAC. Paris, 2002. 2807—2809
19 Bowser G F, Husemann R C. Port Technology International, 1999, **9**: 79—82
20 Bowser G F, Husemann R C. Port Technology International, 2000, **11**: 69—72
21 Bowser G F, Husemann R C. Port Technology International, 2000, **12**: 173—176
22 Bowser G F, Husemann R C. Port Technology International, 2001, **13**: 209—213
23 Elyan V V, Bekhtev B V, Bowser G F et al. PCT Patent, 2004, WO 2004/030162 A2
24 Bjorkholm P J. Port Technology International, 2004, **22-6/4**: 1—3
25 Bjorkholm P J. PCT Patent, 2005, WO 2005/084352 A2
26 Physical Reference Data. National Institute of Standards and Technology. http://physics.nist.gov/PhysRefData/XrayMassCoef/cover.html
27 Grodzins L, Rothschild P. PCT Patent, 2001, WO 01/059485 A1

高能X射线双能成像法中的物质识别

王学武[1)]　李荐民　康克军　唐传祥　张丽　陈志强　李元景　钟华强

(清华大学工程物理系　北京　100084)

摘要　研究了边界能量为1—10MeV的高能X射线成像系统中采用双能成像法识别物质问题. 通过研究其物理机理, 提出了一个近似线性的数学模型; 定义了物质识别灵敏度用于评价物质识别效果; 发现了双能X射线的最优能谱分布区间. 提出并验证了面向最优能谱分布区间的双能X射线能谱调制方法, 大大提高了物质识别灵敏度, 并较好解决了不易识别薄物质的问题. 建成了9MeV/6MeV交替双能成像实验样机, 获得了物质识别着色图像. 相关实验研究结果与理论研究符合得很好.

关键词　高能X射线成像　双能成像　物质识别　电子直线加速器　能谱调制

2007 – 03 – 14 收稿

1) E-mail: wangxuewu@tsinghua.edu.cn